UFR DE MÉDECINE
ET DES PROFESSIONS PARAMÉDICALES
Université Clermont Auvergne

N°

UNIVERSITÉ CLERMONT AUVERGNE

UFR DE MÉDECINE ET DES PROFESSIONS PARAMÉDICALES

THÈSE D'EXERCICE

pour le

DIPLÔME D'ÉTAT DE DOCTEUR EN MÉDECINE

par

OTMAN Hosameldin

Présentée et soutenue publiquement le 23 Octobre 2020

Differential diagnosis between progression and radionecrosis in brain metastases after stereotactic radiosurgery using hybrid FDG-PET and MRI coregistered images

Directrice de thèse : Mme CHANCHOU Marion, Docteur, UFR de Médecine et des professions paramédicales de Clermont-Ferrand

Président du jury : M CACHIN Florent, Professeur, Centre de Lutte contre le Cancer Jean Perrin (Service de Médecine Nucléaire)

Membres du jury :
M DURANDO Xavier, Professeur, UFR de Médecine et des professions paramédicales de Clermont-Ferrand.
M LEMAIRE Jean Jacques, Professeur, UFR de Médecine et des professions paramédicales de Clermont-Ferrand.

UFR DE MÉDECINE
ET DES PROFESSIONS PARAMÉDICALES
Université Clermont Auvergne

N°

UNIVERSITÉ CLERMONT AUVERGNE

UFR DE MÉDECINE ET DES PROFESSIONS PARAMÉDICALES

THÈSE D'EXERCICE

pour le

DIPLÔME D'ÉTAT DE DOCTEUR EN MÉDECINE

par

OTMAN Hosameldin

Présentée et soutenue publiquement le 23 Octobre 2020

Differential diagnosis between progression and radionecrosis in brain metastases after stereotactic radiosurgery using hybrid FDG-PET and MRI coregistered images

Directeur de thèse : Mme CHANCHOU Marion, Docteur, UFR de Médecine et des professions paramédicales de Clermont-Ferrand

Président du jury : M CACHIN Florent, Professeur, Centre de Lutte contre le Cancer Jean Perrin (Service de Médecine Nucléaire)

Membres du jury :
M DURANDO Xavier, Professeur, UFR de Médecine et des professions paramédicales de Clermont-Ferrand.
M LEMAIRE Jean Jacques, Professeur, UFR de Médecine et des professions paramédicales de Clermont-Ferrand.

UFR DE MÉDECINE
ET DES PROFESSIONS PARAMÉDICALES
Université Clermont Auvergne

UNIVERSITÉ CLERMONT AUVERGNE

PRESIDENTS HONORAIRES UNIVERSITE D'AUVERGNE :
JOYON Louis - DOLY Michel - TURPIN Dominique - VEYRE Annie - DULBECCO Philippe - ESCHALIER Alain
PRESIDENTS HONORAIRES UNIVERSITE BLAISE PASCAL :
CABANES Pierre - FONTAINE Jacques - BOUTIN Christian - MONTEIL Jean-Marc - ODOUARD Albert - LAVIGNOTTE Nadine
PRESIDENT DE L'UNIVERSITE et PRESIDENT DU CONSEIL ACADEMIQUE PLENIER :
BERNARD Mathias
PRESIDENT DU CONSEIL ACADEMIQUE RESTREINT :
DEQUIEDT Vianney
VICE-PRESIDENT DU CONSEIL D'ADMINISTRATION :
WILLIAMS Benjamin
VICE-PRESIDENT DE LA COMMISSION DE LA RECHERCHE :
HENRARD Pierre
VICE PRESIDENTE DE LA COMMISSION DE LA FORMATION ET DE LA VIE UNIVERSITAIRE :
PEYRARD Françoise
DIRECTEUR GENERAL DES SERVICES :
PAQUIS François

UFR DE MEDECINE ET DES PROFESSIONS PARAMEDICALES

DOYENS HONORAIRES :
DETEIX Patrice - CHAZAL Jean
DOYEN :
CLAVELOU Pierre
RESPONSABLE ADMINISTRATIVE :
ROBERT Gaëlle

LISTE DU PERSONNEL ENSEIGNANT

PROFESSEURS HONORAIRES :
MM. BACIN Franck - BEGUE René-Jean - BOUCHER Daniel - BOURGES Michel - BUSSIERE Jean-Louis - CANO Noël - CASSAGNES Jean - CATILINA Pierre - CHABANNES Jacques – CHAZAL Jean - CHIPPONI Jacques - CHOLLET Philippe - COUDERT Jean - DASTUGUE Bernard - DEMEOCQ François - DE RIBEROLLES Charles - ESCANDE Georges - Mme FONCK Yvette - MM. GENTOU Claude - GLANDDIER Gérard - Mmes GLANDDIER Phyllis - LAVARENNE Jeanine - MM. LAVERAN Henri - LEVAI

Jean-Paul - MAGE Gérard - MALPUECH Georges - MARCHEIX Jean-Claude - MICHEL Jean-Luc - MOLINA Claude - MONDIE Jean-Michel - PERI Georges - PETIT Georges - PHILIPPE Pierre - PLAGNE Robert - PLANCHE Roger - PONSONNAILLE Jean - RAYNAUD Elie - REY Michel - Mme RIGAL Danièle - MM. ROZAN Raymond - SCHOEFFLER Pierre - SIROT Jacques - SOUTEYRAND Pierre - TANGUY Alain - TERVER Sylvain - THIEBLOT Philippe - TOURNILHAC Michel - VANNEUVILLE Guy - VIALLET Jean-François - Mle VEYRE Annie

PROFESSEURS EMERITES :
MM. - BEYTOUT Jean - BOITEUX Jean-Paul - BOMMELAER Gilles - CHAMOUX Alain - DAUPLAT Jacques - DETEIX Patrice - ESCHALIER Alain - IRTHUM Bernard - JACQUETIN Bernard - KEMENY Jean-Louis – Mme LAFEUILLE Hélène – MM. LEMERY Didier - LESOURD Bruno - LUSSON Jean-René - RIBAL Jean- Pierre

PROFESSEURS DES UNIVERSITES-PRATICIENS HOSPITALIERS

PROFESSEURS DE CLASSE EXCEPTIONNELLE :
M. VAGO Philippe : Histologie-Embryologie Cytogénétique
M. AUMAITRE Olivier : Médecine Interne
M. LABBE André : Pédiatrie
M. AVAN Paul : Biophysique et Traitement de l'Image
M. DURIF Franck : Neurologie
M. BOIRE Jean-Yves : Biostatistiques, Informatique Médicale et Technologies de Communication
M. BOYER Louis : Radiologie et Imagerie Médicale option Clinique
M. POULY Jean-Luc : Gynécologie et Obstétrique
M. CANIS Michel : Gynécologie-Obstétrique
Mme PENAULT-LLORCA Frédérique : Anatomie et Cytologie Pathologiques
M. BAZIN Jean-Etienne : Anesthésiologie et Réanimation Chirurgicale
M. BIGNON Yves Jean : Cancérologie option Biologique
M. BOIRIE Yves : Nutrition Humaine
M. CLAVELOU Pierre : Neurologie
M. DUBRAY Claude : Pharmacologie Clinique
M. GILAIN Laurent : O.R.L.
M. LEMAIRE Jean-Jacques : Neurochirurgie
M. CAMILLERI Lionel : Chirurgie Thoracique et Cardio-Vasculaire
M. DAPOIGNY Michel : Gastro-Entérologie
M. LLORCA Pierre-Michel : Psychiatrie d'Adultes
M. PEZET Denis : Chirurgie Digestive
M. SOUWEINE Bertrand : Réanimation Médicale
M. BOISGARD Stéphane : Chirurgie Orthopédique et Traumatologie
M. CONSTANTIN Jean-Michel : Anesthésiologie et Réanimation Chirurgicale
Mme DUCLOS Martine : Physiologie
M. SCHMIDT Jeannot : Thérapeutique

PROFESSEURS DE 1ère CLASSE :

M. DECHELOTTE Pierre : Anatomie et Cytologie Pathologique
M. CAILLAUD Denis : Pneumo-phtisiologie
M. VERRELLE Pierre : Radiothérapie option Clinique
M. CITRON Bernard : Cardiologie et Maladies Vasculaires
M. D'INCAN Michel : Dermatologie -Vénéréologie
Mme JALENQUES Isabelle : Psychiatrie d'Adultes
Mle BARTHELEMY Isabelle : Chirurgie Maxillo-Faciale
M. GARCIER Jean-Marc : Anatomie-Radiologie et Imagerie Médicale
M. GERBAUD Laurent : Epidémiologie, Economie de la Santé et Prévention
M. SOUBRIER Martin : Rhumatologie
M. TAUVERON Igor : Endocrinologie et Maladies Métaboliques
M. MOM Thierry : Oto-Rhino-Laryngologie
M. RICHARD Ruddy : Physiologie
M. RUIVARD Marc : Médecine Interne
M. SAPIN Vincent : Biochimie et Biologie Moléculaire
M. BAY Jacques-Olivier : Cancérologie
M. BERGER Marc : Hématologie
M. COUDEYRE Emmanuel : Médecine Physique et de Réadaptation
Mme GODFRAIND Catherine : Anatomie et Cytologie Pathologiques
M. ROSSET Eugénio : Chirurgie Vasculaire
M. ABERGEL Armando : Hépatologie
M. LAURICHESSE Henri : Maladies Infectieuses et Tropicales
M. TOURNILHAC Olivier : Hématologie
M. CHIAMBARETTA Frédéric : Ophtalmologie
M. FILAIRE Marc : Anatomie – Chirurgie Thoracique et Cardio-Vasculaire
M. GALLOT Denis : Gynécologie-Obstétrique
M. GUY Laurent : Urologie
M. TRAORE Ousmane : Hygiène Hospitalière
M. ANDRE Marc : Médecine Interne
M. BONNET Richard : Bactériologie, Virologie
M. CACHIN Florent : Biophysique et Médecine Nucléaire
M. COSTES Frédéric : Physiologie
M. FUTIER Emmanuel : Anesthésiologie-Réanimation
Mme HENG Anne-Elisabeth : Néphrologie
M. MOTREFF Pascal : Cardiologie
Mme PICKERING Gisèle : Pharmacologie Clinique

PROFESSEURS DE 2ème CLASSE :

Mme CREVEAUX Isabelle : Biochimie et Biologie Moléculaire
M. FAICT Thierry : Médecine Légale et Droit de la Santé
Mme KANOLD LASTAWIECKA Justyna : Pédiatrie
M. TCHIRKOV Andréï : Cytologie et Histologie
M. CORNELIS François : Génétique
M. DESCAMPS Stéphane : Chirurgie Orthopédique et Traumatologique
M. POMEL Christophe : Cancérologie – Chirurgie Générale
M. CANAVESE Fédérico : Chirurgie Infantile

M. LESENS Olivier : Maladies Infectieuses et Tropicales
M. RABISCHONG Benoît : Gynécologie Obstétrique
M. AUTHIER Nicolas : Pharmacologie Médicale
M. BROUSSE Georges : Psychiatrie Adultes/Addictologie
M. BUC Emmanuel : Chirurgie Digestive
M. CHABROT Pascal : Radiologie et Imagerie Médicale
M. LAUTRETTE Alexandre : Néphrologie Réanimation Médicale
M. AZARNOUSH Kasra : Chirurgie Thoracique et Cardiovasculaire
Mme BRUGNON Florence : Biologie et Médecine du Développement et de la Reproduction
Mme HENQUELL Cécile : Bactériologie Virologie
M. ESCHALIER Romain : Cardiologie
M. MERLIN Etienne : Pédiatrie
Mme TOURNADRE Anne : Rhumatologie
M. DURANDO Xavier : Cancérologie
M. DUTHEIL Frédéric : Médecine et Santé au Travail
Mme FANTINI Maria Livia : Neurologie
M. SAKKA Laurent : Anatomie – Neurochirurgie
M. BOURDEL Nicolas : Gynécologie-Obstétrique
M. GUIEZE Romain : Hématologie
M. POINCLOUX Laurent : Gastroentérologie
M. SOUTEYRAND Géraud : Cardiologie

PROFESSEURS DES UNIVERSITES

M. CLEMENT Gilles : Médecine Générale
Mme MALPUECH-BRUGERE Corinne : Nutrition Humaine
M. VORILHON Philippe : Médecine Générale

PROFESSEURS ASSOCIES DES UNIVERSITES

Mme BOTTET-MAULOUBIER Anne : Médecine Générale
M. CAMBON Benoît : Médecine Générale

MAITRES DE CONFERENCES DES UNIVERSITES - PRATICIENS HOSPITALIERS

MAITRES DE CONFERENCES HORS CLASSE
Mme CHAMBON Martine : Bactériologie Virologie
Mme BOUTELOUP Corinne : Nutrition

MAITRES DE CONFERENCES DE 1ère CLASSE
M. MORVAN Daniel : Biophysique et Traitement de l'Image
Mle GOUMY Carole : Cytologie et Histologie, Cytogénétique

Mme FOGLI Anne : Biochimie Biologie Moléculaire
Mle GOUAS Laetitia : Cytologie et Histologie, Cytogénétique
M. MARCEAU Geoffroy : Biochimie Biologie Moléculaire
Mme MINET-QUINARD Régine : Biochimie Biologie Moléculaire
M. ROBIN Frédéric : Bactériologie
Mle VERONESE Lauren : Cytologie et Histologie, Cytogénétique
M. DELMAS Julien : Bactériologie
Mle MIRAND Andrey : Bactériologie Virologie
M. OUCHCHANE Lemlih : Biostatistiques, Informatique Médicale et Technologies de Communication
M. LIBERT Frédéric : Pharmacologie Médicale
Mle COSTE Karen : Pédiatrie
M. EVRARD Bertrand : Immunologie
Mle AUMERAN Claire : Hygiène Hospitalière
M. POIRIER Philippe : Parasitologie et Mycologie
Mme CASSAGNES Lucie : Radiologie et Imagerie Médicale
M. LEBRETON Aurélien : Hématologie

MAITRES DE CONFERENCES DE 2ème CLASSE

Mme PONS Hanaë : Biologie et Médecine du Développement et de la Reproduction
M. JABAUDON-GANDET Matthieu : Anesthésiologie – Réanimation Chirurgicale
M. BOUVIER Damien : Biochimie et Biologie Moléculaire
M. BUISSON Anthony : Gastroentérologie
M. COLL Guillaume : Neurochirurgie
Mme SARRET Catherine : Pédiatrie
M. MAQDASY Salwan : Endocrinologie, Diabète et Maladies Métaboliques
Mme NOURRISSON Céline : Parasitologie – Mycologie

MAITRES DE CONFERENCES DES UNIVERSITES

Mme BONHOMME Brigitte : Biophysique et Traitement de l'Image
Mme VAURS-BARRIERE Catherine : Biochimie Biologie Moléculaire
M. BAILLY Jean-Luc : Bactériologie Virologie
Mle AUBEL Corinne : Oncologie Moléculaire
M. BLANCHON Loïc : Biochimie Biologie Moléculaire
Mle GUILLET Christelle : Nutrition Humaine
M. BIDET Yannick : Oncogénétique
M. MARCHAND Fabien : Pharmacologie Médicale
M. DALMASSO Guillaume : Bactériologie
M. SOLER Cédric : Biochimie Biologie Moléculaire
M. GIRAUDET Fabrice : Biophysique et Traitement de l'Image
Mme VAILLANT-ROUSSEL : Hélène Médecine Générale
Mme LAPORTE Catherine : Médecine Générale
M. LOLIGNIER Stéphane : Neurosciences – Neuropharmacologie
Mme MARTEIL Gaëlle : Biologie de la Reproduction
M. PINEL Alexandre : Nutrition Humaine

MAITRES DE CONFERENCES ASSOCIES DES UNIVERSITES

M. TANGUY Gilles : Médecine Générale
M. BERNARD Pierre : Médecine Générale
Mme ESCHALIER Bénédicte : Médecine Générale
Mme RICHARD Amélie : Médecine Générale

Au président du jury,

A Monsieur le Professeur Florent CACHIN

Pour m'avoir fait l'honneur d'accepter de présider ce jury et de juger ce travail. Vos connaissances et votre précision dans le travail vous honorent.

Soyez assuré de ma reconnaissance et de mon respect éternel.

A la directrice de cette thèse,

A Madame le Docteur Marion CHANCHOU

Pour m'avoir guidé dans ce travail. Merci de m'avoir accompagné tout au long de mon internat et de m'avoir fait partager tes connaissances. Merci aussi pour ta gentillesse et ton soutien, ce fut toujours un plaisir de travailler avec toi.

Aux membres de mon jury,

A Monsieur le Professeur Xavier DURANDO

Pour l'honneur que vous m'avez fait de participer à ce jury et d'y apporter votre point de vue clinique.

Je vous prie de croire en l'expression de ma profonde considération.

A Monsieur le Professeur Jean Jacques LEMAIRE

Pour l'honneur que vous m'avez fait en acceptant de juger cette thèse et d'y apporter votre expertise. Je vous remercie pour cette précieuse collaboration entre nos deux spécialités.

Soyez assuré de ma considération respectueuse.

Remerciements

Je remercie mes parents pour leur soutien inconditionnel durant toute cette histoire, et je sais que je peux compter sur leur soutien et leur amour pour les autres aventures à venir.

Je remercie mon frère, le bro des enfers. Come back here Venom! Where are you?

A ma douce Audrey qui a gentiment accepté de me fréquentater. Et c'est sympa.

A Paul, le Gaju de tous les Gaju. You da real mvp.

A Adrien, mon "compagnon" de philosophie et de dégustation de mets raffinés.

Au gang des externes nîmois et leur indéfectible soutien (et tolérance pour mes bêtises) : Florent (mon fils!), Bastien, Sarah, Grégoire (<3).

A la guilde des montpelliérains, des amis inestimables que je ne vois pas assez souvent à mon goût : jvous aime p****n!

Raphaël, wished I knew you one life ago.

A Gilles, mon chou adoré!

Fidji, une amie irremplaçable et fidèle. La ville de Lille a vraiment de la chance de t'avoir !

Je remercie toute l'équipe de mon service de Médecine Nucléaire du Centre Jean Perrin, qui a sû tolérer (ou s'habituer) mon caractère et que je suis heureux de rejoindre en tant qu'assistant.

Je remercie les professionnels qui m'ont enseigné mes cours de flûte et de lancer de saucisses.

Big up à ma promotion de Saclay, très probablement la meilleure de toutes.

Liste des abréviations

BM : Brain metastasis

SRS : Stereotaxic radiosurgery

WBRT : Whole brain radiotherapy

TR : Tumor recurrence

TP : Tumor progression

ROI : Region of interest

FDG : [^{18}F]fluorodeoxyglucose

PET/CT : Positron emission tomography–computed tomography

MRI : Magnetic resonance imaging

OS : Overall survival

PFS : Progression free survival

WM : White matter

AUC : Area Under Curve

FDR : False Discovery Rate

Introduction

The frequency of brain metastasis (BM) is continuously increasing in developed countries(1). While radiation therapy remains the standard treatment for non-surgical lesions(2), we are currently observing a shift in practices in favor of stereotactic radiosurgery (SRS) instead of whole-brain radiotherapy (WBRT), presenting a good performance with a decreased neurotoxicity (3). One of the most frequent clinical and radiological complication is radiation injury(4,5), which can be divided into two categories : “pseudo-progression”, a short-term subacute brain injury occurring within the first weeks of treatment; and “radiation necrosis” (RN), a late occurring condition that can remain from months up to years(6). Radiation necrosis usually appears within the same period as tumor progression (TP) and displays the same radiological presentation on MRI(6), both of them appearing as an enlarged and contrast-enhanced lesion due to the blood-brain barrier breakdown in both conditions(2,7). Multiparametric MRI offers useful tools that can guide and help the radiologist, but these non-universally available techniques are often criticized for their lack of reproducibility(8). While brain biopsy remains the gold standard, it is a highly invasive technique which brings out many concerns (tumor localization, performance status, patient willingness, cost limits) and often remains a last case option(8,9). In this situation, brain positron emission tomography with computed tomography (PET/CT) using [^{18}F]fluorodeoxyglucose (FDG) may provide additional diagnostic arguments to help clinical decision(7,10).

A dual-phase protocol has been proven helpful to assess FDG-avid tumors (11). In this protocol, a first PET/CT (“early image”) is performed 30 minutes after FDG injection. A second PET/CT (“delayed image”) is acquired(12) 4h hours after the first acquisition. Normal brain tissue, immune system cells and tumor cells have a very different glycolytic metabolism(13), allowing this postulate : the tracer will build up in tumors or tumor

recurrences while its retention remains stable within normal tissue or inflammatory process(13). This will lead to a difference of maximum Standard Uptake Value (SUVmax) in the brain tumor and the background normal brain tissue, with better sound to noise ratio(14), allowing us to determine the lesion retention index (RI).

A few studies and meta-analysis have sought to improve diagnostic performance by associating PET/CT and MRI with interesting results but many biases, mostly within image post-processing (15). Coregistered MRI and dual phase PET/CT (PET) images could be used to extract prognostic biomarkers. Such parameters could help distinguish between TP and RN and stratify patients with better overall survival (OS) and progression-free survival (PFS), standard criteria in cancer treatment evaluation (2,14).

The aim of this study was to extract MRI and dual phase PET biomarkers associated with TP or RN in patients treated by SRS for BM using coregistered images for quantitative analysis. On secondary analysis, we also conducted a semi-quantitative and a visual analysis to assess the performance of both MRI and PET.

Methods

Study Population

Fifteen patients were retrospectively included from January 2018 to September 2020 from two hospitals : the University Hospital of Montpellier and the Jean Perrin Center of Clermont Ferrand (France). Inclusion criteria were as follow: patients older than 18 years, anatomopathological proven primary disease and history knowledge of a brain metastasis, treatment with stereotactic radiosurgery, development during follow-up of a contrast-enhanced MRI lesion with non-conclusive definitive diagnostic for tumor progression according to the local multidisciplinary neuro oncological board which led to a dual-phase brain FDG PET/CT (PET). Exclusion criteria were pregnancy, contraindications to MRI or PET imaging or contraindications to contrast agent administration. The authorization from both hospitals local ethical committees was obtained. Written consentment was obtained from each patient.

PET/CT and MRI Imaging Technics

After a minimum of 6 hours fasting, patients were installed on a either a BIOGRAPH mCT-20 Flow-4R SIEMENS (Montpellier) or a Discovery 710 Optima 660 or Discovery MIDR General Electrics (Clermont Ferrand) for a brain acquisition. The patients were injected intravenously with 125–250 MBq (typically 150 MBq) of ^{18}F-FDG followed by an “early acquisition” 30 minutes after injection. The “delayed image” was acquired 4 hours after the injection. Low dose non-contrast enhanced CT scan was acquired for anatomic localization and attenuation correction. All PET images reconstruction that includes corrections for scatter, random events, dead time, and attenuation (from CT) were obtained with OSEM (10 iteration and 32 subsets) + TOF (VUE Point FX) algorithm using a standard Z cutoff filter and 5 mm frequency cut including point spread function modelling (SharpIR).

The usual brain tumor MRI protocol (before and after intravenous gadolinium contrast, in adequation with the guidelines(16)) was performed on a 3T MRI (Skyra 3T and Prisma 3T, Siemens, Erlangen, Germany). The reconstruction parameters can be found in Annexe 1. A 0.2 mL/kg bolus of contrast agent was administered at 6 mL/s. The contrast agent used depended on the patient: either Gd-DOTA, gadoterate meglumine, Dotarem® (Guerbet, France) or Gd-BOPTA, gadobenate dimeglumine, MultiHance® (Bracco Imaging SpA, Milan, Italy).

A minimum period of 3 months separated the last SRS session from the imaging acquisitions.

Image Analysis

Coregistration quantitative analysis

Perfusion maps were generated with Olea Sphere 3.0 (Olea Medical® SA, Toshiba Medical Systems Corporation) using a block-circulant singular value decomposition (CSVD) deconvolution. We devised a Matlab script (The MathWorks Inc. MATLAB, Massachusetts, United States) using SPM12 toolbox (Statistical Parametric Mapping (17)) to convert the permeability cartography. The contrast-enhanced T1 MPRAGE images of each patient were reoriented on the anterior commissure, then all images were coregistered on the contrast-enhanced T1 MPRAGE images using Matlab and SPM12(28). Every metric was then statistically explored to find its association with either diagnostic.

Tumor localization and 3D (ROI) were devised using MRIcron software (Chris Rorden's MRIcron (18)) by an experienced resident with the supervision of two experienced senior radiologists. Semi-automated ROIs were drawn on the tumor on the axial T1 MRI, H1 and H4 PET images; a reference contralateral white-matter spheric ROI was also drawn for

standardization. The ROIs were named : **MRI** (ROI drawn on the T1 MPRAGE images), **Early** (ROI drawn on the early one hour PET), **Delayed** (ROI drawn on the delayed four hour PET) and **WM** (ROI drawn on contralateral white matter). Perfusion and permeability metrics (on MRI sequences) were recorded inside these ROIs.

For the MRI metrics, every metric was evaluated for their association with either diagnostic, with the metric alone and the standardized metric which was defined by the ratio **MRI**/**WM** (the ROI drawn on the tumor / the contralateral white matter ROI). For the PET, we measured the SUVmax inside the ROIs (Early, Delayed and WM) and calculated the same metrics as in the semi-quantitative analysis, on the early (**Early/WM**) and delayed acquisition (**Delayed/WM**) and also the Retention Index (see below in Semi-Quantitative analysis).

Semi-quantitative analysis

PET and MRI were analysed by experimented radiologists (for MRI) and nuclear physicists (for PET); tumor localizations were noted. On dual phase PET, maximum standardized uptake values (SUVmax) of the lesion (L) were measured at “early” (1) and “delayed” (2) imaging acquisitions (using a 40% cut-off). A mirror contralateral region of interest (ROI) was used as standardization (WM for White Matter). Ratios of L SUVmax to WM SUVmax at “early” and “delayed” time points (L1/WM1 and L2/WM2 respectively) were calculated individually, and the change between early and late L to WM ratios was calculated using the formula: [(L2/ GM2 - L1/GM1)/(L1/GM1)] (19). This ratio was called the Retention Index (RI). A 20% increase in this RI was considered as TR, whereas a change of RI less than 10% was not significant and was in favor of RN.

Visual analysis

On a secondary visual analysis, each PET acquisition (early and delayed) was also randomly analysed by an experienced resident, blindly to the results of the other acquisition for the same patient. The resident then interpreted the combined images of the early and delayed acquisitions. A binary subjective fixation score was used to assess each lesion, as "suspicious" or "non suspicious" of progression. This was to investigate if a reliable and robust diagnostic could be obtained with either one of the modalities (early or delayed acquisition) instead of interpreting both of them (combined interpretation of both early and delayed acquisitions).

Follow-up analysis

Demographic features (age, sexe…) were noted. Every patient had a minimum of 6 months follow up. Additional treatments before and after baseline imaging were noted, including chemotherapy, corticosteroids and anti-VEGF monoclonal antibodies such as bevacizumab, which have been proven to be an effective treatment option for symptomatic radionecrosis (20,21). Patients follow up usually consisted of a routine MR imaging every 2 months followed by a neurological clinical assessment.

The gold standard was the decision of the neuro oncological committee; patients were retrospectively sorted whether they had tumor progression or radionecrosis, based on multiple radiological, clinical and histological criteria(when biopsy was performed). Such composite score has been used in many similar studies (19) and is truly a reflection of daily practice.

Statistical analysis

The statistical significance threshold used was 0,05. Since a large number of tests was performed (n = 47), the Benjamini-Hochberg method was at first considered in order to adjust the p-values. The tests used to compare the distributions between the groups was Welsh's t test or the Wilcoxon-Mann- Whitney test (depending on the distribution of the data). ROC curves were computed, along with AUC, for the variables having obtained a p-value < .05. For the evaluation of the performance of the classifiers, we computed a set of statistics on the contingency tables. Statistical analysis was performed on R-software, version 3.6.1 (R-Project, GNU GPL, http ://cran.r-project.org/).

Results

Patient Characteristics

Fifteen patients matching the inclusion criteria were included (male:female = 6:9, mean age 64,36 years; SD 8,71; range 49-78). Main tumoral locations were as follows : frontal (ten patients), parietal (two patients), temporal (two patients) et cerebellum (one patient). The primary tumor was a lung neoplasm in fourteen patients and breast cancer in one patient. Two patients had a surgical resection followed by a stereotactic radiosurgery on the tumoral bed. No additional treatment was introduced between the last SRS session and the MRI / PET.

Table I : Patients and lesion characteristics

TABLE I : Patient and lesion characteristics	
Characteristics	**Values**
Number of patients	15
Final diagnosis :	
Tumor Progression	9 (60%)
Radionecrosis	6 (40%)
Gender	male:female = 6:9
Age	64,36 years; SD 8,71; range 49-78
Histological confirmation	8 (53%)
Brain Metastasis Location :	
Frontal	10 (67%)
Temporal	2 (13,33%)
Parietal	2 (13,33%)
Cerebellum	1 (6,7%)
Primitive :	
Lung carcinoma	14 (93%)
Breast carcinoma	1 (6,67%)

After follow up, 9 patients were ruled out as tumor progression and 6 patients as radionecrosis. In these nine patients in progression, histological diagnosis was obtained in eight patients. The seventh patient also had a new adrenal localization; the oncological committee therefore proposed a chemotherapy. There was no histological confirmation for patients of the radionecrosis group; whose diagnosis was confirmed on patient follow up. Two examples can be found in Figure 1 and Figure 2.

Figure 1

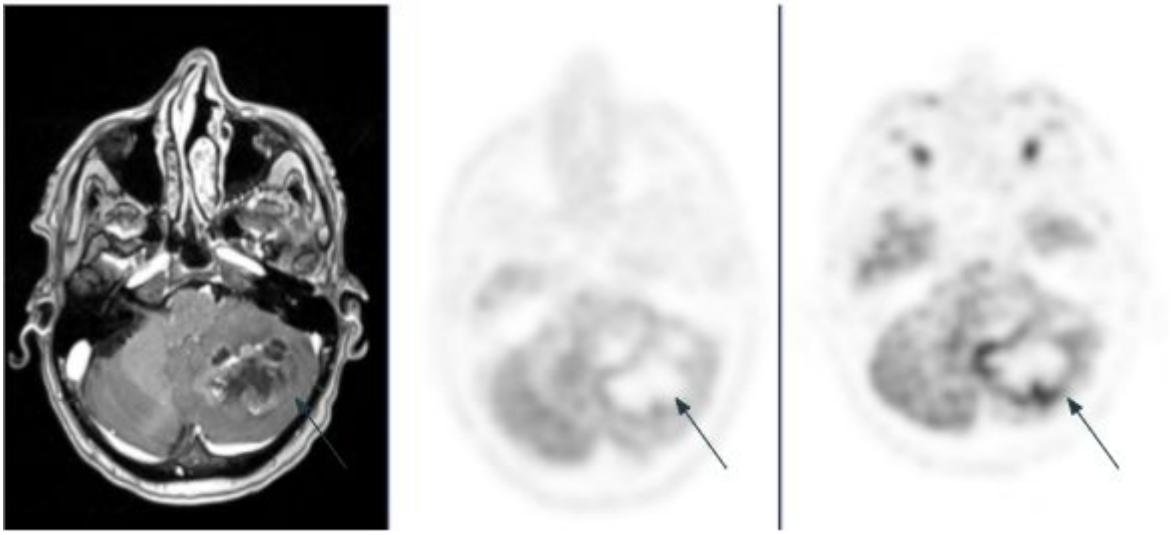

Illustration of a tumor progression : T1 Gado MRI (left), early (middle) and delayed (right) dual phase brain FDG PET/CT images. The SUVmax of the contrast enhanced lesion in the left cerebellum (arrow) increased by 80% in comparison to the normal contralateral gray matter. This was later confirmed by a control MRI and surgery.

Figure 2

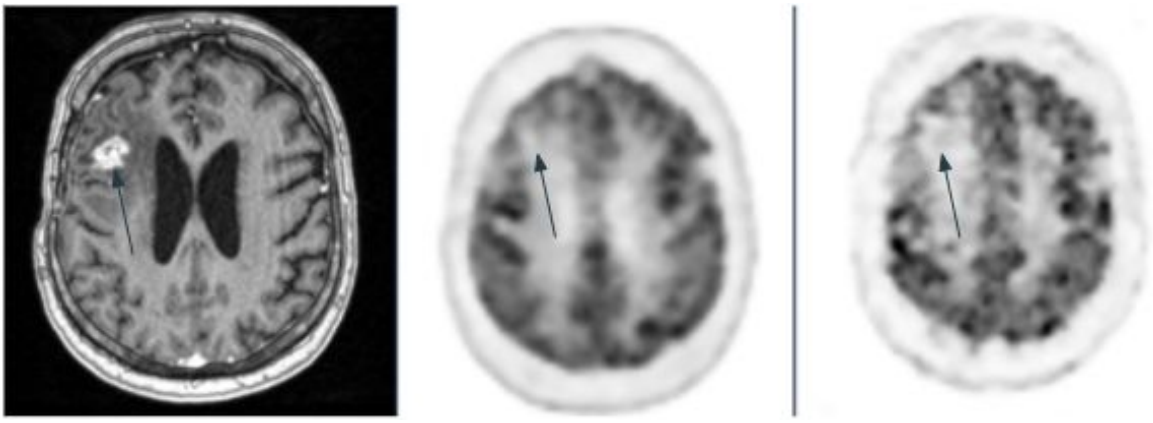

Illustration of a radionecrosis : T1 Gado MRI (left), early (middle) and delayed (right) dual phase brain FDG PET/CT images. There's a very low uptake on the right frontal lesion (arrow) which decreases on delayed images. The SUVmax ratio decreased by 9%, consistent with radionecrosis. MRI serial follow-up demonstrated lesion stability.

Coregistration quantitative analysis

We measured every metric inside the measured ROIs when the sequences were available and can be found in their entirety in Annexe 2. When considering the metrics inside the MRI drawn ROIs, there was no statistically significant difference between TR and TP groups. When standardized on WM (Table II), there was a statistically significant difference between the two groups for three MRI metrics : VP (mean plasma volume, a perfusion metric; p = 0,042 ; 95% CI [-2.68 – -0.07]), Washin (wash-in rate of contrast into the tissue; p = 0,037 ; 95% CI [(-1.61 – -0.09]) and PeakEnhancement (p = 0,037 ; 95% CI [-3.71 – -0.16]). There was a strong statistically significant difference between the two groups for two PET metrics : the Delayed/WM ratio (p = 0,008) ; 95% CI [0.33 – 1.67]) and the Retention Index (RI) (p = 0,016 ; 95% CI [0.14 – 1.1]). However, this small sample generated a lack of statistical power, thus requiring a FDR-controlling procedure (False Discovery Rate) with a Benjamini–Hochberg procedure. After adjustment, there was no statistically significant difference between the groups. However, the study being weakly powered because of the

small sample sizes in each group (n = 9, et 6, respectively), and the presence of missing data (for some of the MRI metrics), the multiple testing correction turned out to be too conservative, as expected.

Table II : Coregistration quantitative analysis

Variable	Progression group	Radionecrosis group	Estimation*	95% CI	p	Adjusted p-value	Test*
ROI MRI / WM VP	**2.10**	**3.48**	**-1.38**	**(-2.68 -- -0.07)**	**.042**	**.391**	**Welch**
ROI MRI / WM Washin	**1.45**	**2.30**	**-0.85**	**(-1.61 -- -0.09)**	**.035**	**.391**	**Welch**
ROI MRI / WM PeakEnhancement	**2.66**	**4.60**	**-1.94**	**(-3.71 -- -0.16)**	**.037**	**.391**	**Welch**
ROI Delayed / WM	**2.10**	**1.10**	**1.00**	**(0.33 -- 1.67)**	**.008**	**.361**	**Welch**
Retention Index	**0.72**	**0.10**	**0.62**	**(0.14 -- 1.1)**	**.016**	**.374**	**Welch**

*The colon Est is an estimation of the median of the differences (in case of a Wilcoxon-Mann-Whitney test) or the differences of the means (in case of a Welsh test) between the two groups tumor progression and radionecrosis.
Differences with statistical significance (α = .05) are in bold.
ROIs : **MRI** (ROI drawn on the T1 MPRAGE images), **Early** (ROI drawn on the early one hour PET), **Delayed** (ROI drawn on the delayed four hour PET) and **WM** (ROI drawn on contralateral white matter)
No : Number of metric
No 1 to 22 : metric recorded inside the **MRI** ROI, drawn on the T1 MPRAGE images
No 23 to 44 : standardized metrics **MRI** / **ROI**
Retention Index = [(**Delayed**/**WM** - **Early**/**WM**)/(**Early**/**WM**)]

Figure 3 shows the ROC-derived cut-off values for these statistically significant metrics. The AUC represents the area under the ROC curve, which is a measure of the performance of the metric. The Retention Index was the most sensitive and specific predictors of outcome.

The best threshold according to the Younden index is 0,15 which corresponds to a Sensitivity of 83% and a Specificity of 100% (AUC = 0,94 ; 95% CI [0,82 ; 1]).

Figure 3 : ROC curve analysis

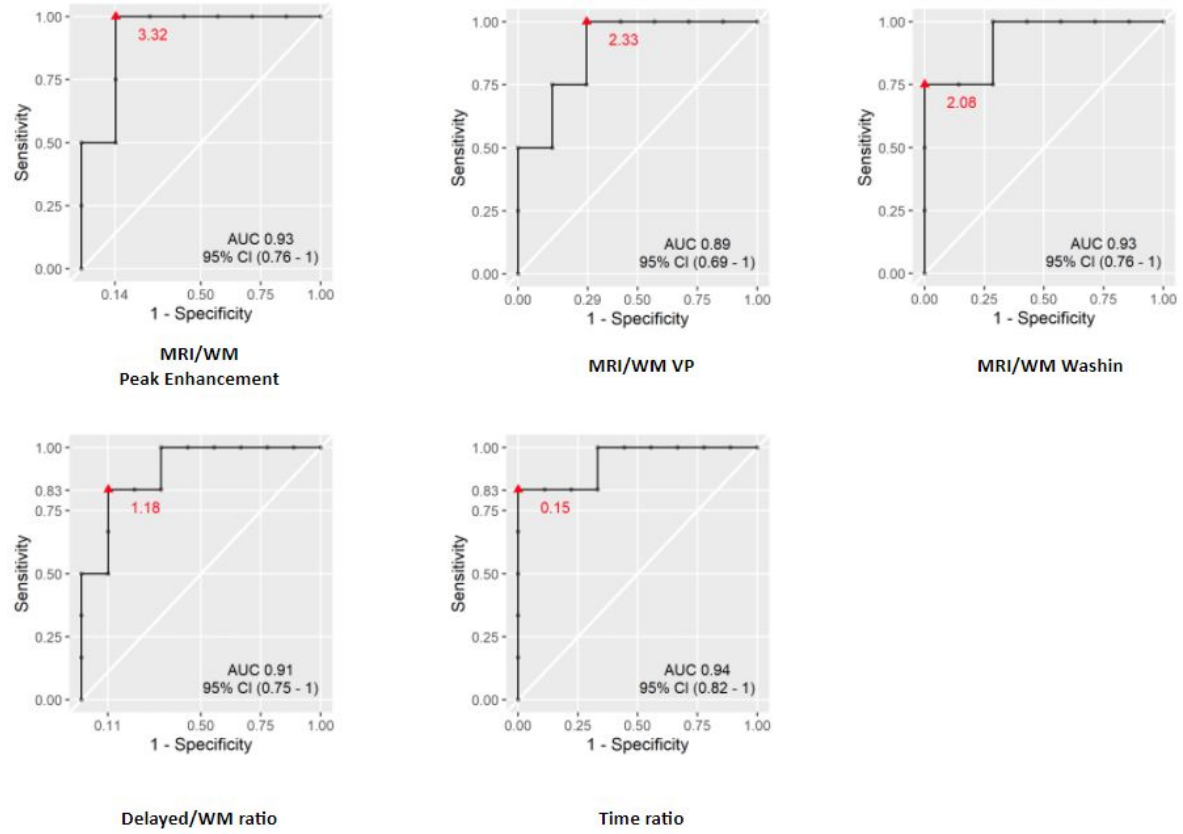

ROC curves for discrimination between tumor progression and radionecrosis for the statistically significant metrics.
ROIs : **MRI** (ROI drawn on the T1 MPRAGE images), **Early** (ROI drawn on the early one hour PET), **Delayed** (ROI drawn on the delayed four hour PET) and **WM** (ROI drawn on contralateral white matter).

Semi-quantitative analysis

On semi-quantitative analysis realized by a senior radiologist (for MRI) or a senior nuclear physician (for PET), PET identified 9 patients with tumor progression and 6 patients with radionecrosis, thus obtaining a 100% Sensitivity and Specificity. MRI identified 8 patients as tumor progression and 7 patients with radionecrosis, thus obtaining a Sensitivity and

Specificity of 87,5 and 85,71 respectively. There were one false negative tumor progression diagnosis and one false positive tumor progression diagnosis on MRI which were subsequently characterized on MRI follow-up and brain biopsy (Table II). On PET semi-quantitative analysis, an increase of 20% or more of the Retention Index was found in every patient ruled out as TR. A change of RI lesser than 10% or a decrease in Retention Index was found in every patient ruled out as RN.

Table III : MRI & PET diagnostic performances

Modality		Final Diagnosis	
		Progression	Radionecrosis
MRI Diagnostic	Progression	7	1
	Radionecrosis	1	5
PET Diagnostic	Progression	9	0
	Radionecrosis	0	6

Visual analysis

The results of the PET visual analysis are shown in Table IV. Random interpretation (i.e. either early or delayed acquisition) or combined interpretation (i.e. combined interpretation of early and delayed acquisition) diagnoses were concordant for every patient, but there was a final diagnostic concordance in 8/15 cases (53%). In those 8 cases, the initial and final diagnosis was in favor of TR in 6 patients and RN for 2 patients. In 9 cases, the random visual interpretation or the combined visual combined interpretation were falsely concordant.

Table IV : Visual analysis

Table IV : Visual analysis					
Patient	Blind analysis		Combined analysis	Final Diagnosis	Diagnostic Concordance
	Early Acquisition	Delayed Acquisition			
1	non suspicious	non suspicious	non suspicious	progression	**No**
2	non suspicious	non suspicious	non suspicious	progression	**No**
3	non suspicious	non suspicious	non suspicious	progression	**No**
4	suspicious	suspicious	suspicious	progression	**Yes**
5	suspicious	suspicious	suspicious	progression	**Yes**
6	suspicious	suspicious	suspicious	radionecrosis	**No**
7	suspicious	suspicious	suspicious	radionecrosis	**No**
8	suspicious	suspicious	suspicious	radionecrosis	**No**
9	suspicious	suspicious	suspicious	progression	**Yes**
10	suspicious	suspicious	suspicious	progression	**Yes**
11	non suspicious	non suspicious	non suspicious	progression	**No**
12	suspicious	suspicious	suspicious	progression	**Yes**
13	non suspicious	non suspicious	non suspicious	radionecrosis	**Yes**
14	non suspicious	non suspicious	non suspicious	radionecrosis	**Yes**
15	suspicious	suspicious	suspicious	progression	**Yes**

Discussion

Conventional imaging alone isn't enough to rule out local recurrence(8). Our study reported excellent diagnostic accuracies for both PET and MRI with findings consistent with literature data(2,5,11–13,22,23); the combined use of PET and MRI data can accurately help the physician, moreover when both studies were concordant. When standardized on WM, the quantitative analysis found interesting results within the different metrics explored on quantitative analysis, with a strong statistical significance. A visual analysis alone didn't seem to prove itself robust enough to obtain a right diagnosis, suggesting again the need for reliable biometrics, such as the Retention Index, which has been proven helpful in both quantitative and semi-quantitative analysis.

Horky et Al retrospectively explored 32 patients with suspicion of tumor progression on the control MRI for brain tumors treated with SRS who underwent dual-phase FDG-PET/CT(19). A modification of the ratio > 0,19 of L/WM ratios was highly effective for differentiating tumor progression versus radionecrosis, with 95 % Sensitivity, 100 Specificity and 96,4% Accuracy. In a similar setting to our study(24), Leiva-Salinas et AL retrospectively analyzed 85 patients and explored whether relative SUV (ratio of SUVmax in the tumor divided by the contralateral SUVmax in healthy white matter) on dual-phase FDG-PET/CT + MRI coregistration could be a biomarker of response in patients who underwent SRS for BM with suspected tumor progression. On multivariate analysis, they found a significant association between relative SUV and tumor progression (p = 0,035).

Pseudo progression and radiation necrosis both display contrast-enhanced lesions on MRI, making it difficult to discriminate between tumor progression or radiation injury. While being the reference, anatomopathological diagnosis is rarely pursued : tumor localization,

invasiveness or the patient's general health often rule out surgical biopsy. There was no histological confirmation of radionecrosis; which was confirmed on patients' follow up. Moreover, the benefit-risk balance may not be enough to justify this procedure, even more so if radionecrosis is the main hypothesis, which explains why there are such a few histologically proven diagnoses of radionecrosis, as the biopsy wouldn't change the treatment(22). A recurrence was histologically proven in 8 out of 9 patients in TR, as one patient also has a new adrenal metastasis. There was no additional treatment introduced between the last SRS session and the two imaging modalities, ensuring again the homogeneity of our population.

We had two PET/MRI discordances. For the first patient, the MRI was in favor of tumor progression whereas the PET (performed one month later) suggested radionecrosis. A brain CT three months later demonstrated a partial regression of the brain lesion which was later confirmed on the control MRI one month later, confirming the radionecrosis. For the second patient, the MRI performed 4 months after the radiotherapy suggested radionecrosis. The PET (performed one month later) was in favor of tumor progression whereas the control MRI (performed one month after the PET) suggested radionecrosis. Two months later, the control MRI and PET were both in favor of tumor progression, which was histologically confirmed.

One of the strengths of this study is its accessibility. Multiparametric MRI and dual phase FDG-PET coregistration is a powerful diagnostic tool and the protocol remains simple and easily transposable. FDG is the most commonly used PET radiotracer in opposition to amino acid PET radiotracers, such as [^{18}F]-DOPA, and [^{18}F]-FET or ^{18}F-fluorocholine(13,25,26), which are as well documented and promising than hardly accessible. In a meta-analysis including

48 studies(27), Yu et al investigated the diagnostic performance of 18 F-FDOPA PET and 18 F-FET PET for differentiating TR and RN, and found for 18F-FDOPA and 18F-FET groups respectively : sensitivity, 0.85 versus 0.82; specificity, 0.77 versus 0.80.

The primary limitation of our study remains its sample size : this small, bi-center retrospective study cannot be applied to the general population, but could be a stepping stone for other projects. We adopted a strict enrollment policy to ensure the robustness of our sample. We tried to enroll the most homogenous population by including only patients referred by the neuro oncological committees if and only if the patient developed a contrast-enhanced image on MRI during follow-up with no definite diagnostic between local recurrence or radionecrosis for a brain metastasis treated with stereotaxic radiosurgery. We did not include any other type of brain neoplasm (gliomas, glioblastomas or lymphomas) to ensure the homogeneity of our sample. MRI and dual phase brain FDG PET/CT were performed for all patients, without any new treatment introduced. Patients were followed at least 6 months after performing both exams.

With one committee of experienced seniors, the diagnostic algorithm was robust but may generate treatment, patient selection and center related biases. In exchange, this provided standardized protocols in terms of surgery planning, radiation delineation and dose delivery. In addition, semi-automated ROIs were drawn by an experimented resident which could be a limitation to this study; these ROIs were all reviewed by two experienced senior neuro-radiologists to contain this bias. Furthermore, the visual analysis didn't prove to be robust enough on either setting (random or combined interpretation), but was only interpreted by a resident experienced in neuroimaging. Finally, our sample size didn't allow

us to evaluate prognosis based data such as overall and/or progression free survival but could be a stepping stone for a future study.

Conclusion

UFR DE MÉDECINE
ET DES PROFESSIONS PARAMÉDICALES
Université Clermont Auvergne

Service de la formation
3ème cycle - Pôle 3

CONCLUSION DE LA THESE

La TEP biphasique discrimine efficacement entre progression tumorale et radionécrose, notamment grace à l'augmentation du ratio de SUVmax qui est un biomarqueur efficace dans cette indication. L'analyse conjointe des données TEP et IRM améliore la précision diagnostique et conforte le clinicien dans sa décision. La corégistration des données TEP et IRM pourrait améliorer le diagnostic. Cette analyse fournit des résultats encourageants mais nécessite une étude plus approfondie avec une plus grande série prospective de patient

Clermont-Ferrand, le 22/09/2020
Pierre CLAVELOU
Doyen - Directeur

Faculté de Médecine Clermont-Ferrand

Clermont-Ferrand, le
Le Président du Jury

Professeur Florent CACHIN
Directeur Scientifique
Responsable Universitaire Département d'Imagerie
PU-PH Médecine nucléaire
RPPS : 10003170320
Centre Jean PERRIN - B.P. 392
63011 CLERMONT-FERRAND cedex 1
France

UFR de Médecine et des Professions Paramédicales
Service de la formation – Pôle 3
TSA 50400
28, Place Henri-Dunant
63001 Clermont-Ferrand Cedex 1

References

1. Sperduto PW, Kased N, Roberge D, Xu Z, Shanley R, Luo X, et al. Summary Report on the Graded Prognostic Assessment: An Accurate and Facile Diagnosis-Specific Tool to Estimate Survival for Patients With Brain Metastases. J Clin Oncol. 2012 Feb 1;30(4):419–25.
2. Hatiboglu MA, Akdur K, Sawaya R. Neurosurgical management of patients with brain metastasis. Neurosurg Rev. 2020 Apr;43(2):483–95.
3. Information NC for B, Pike USNL of M 8600 R, MD B, Usa 20894. A meta-analysis evaluating stereotactic radiosurgery, whole-brain radiotherapy, or both for patients presenting with a limited number of brain metastases [Internet]. Database of Abstracts of Reviews of Effects (DARE): Quality-assessed Reviews [Internet]. Centre for Reviews and Dissemination (UK); 2012 [cited 2020 Sep 28]. Available from: https://www.ncbi.nlm.nih.gov/books/NBK98468/
4. Minniti G, Clarke E, Lanzetta G, Osti MF, Trasimeni G, Bozzao A, et al. Stereotactic radiosurgery for brain metastases: analysis of outcome and risk of brain radionecrosis. Radiat Oncol Lond Engl. 2011 May 15;6:48.
5. Lohmann P, Stoffels G, Ceccon G, Rapp M, Sabel M, Filss CP, et al. Radiation injury vs. recurrent brain metastasis: combining textural feature radiomics analysis and standard parameters may increase 18F-FET PET accuracy without dynamic scans. Eur Radiol. 2017 Jul;27(7):2916–27.
6. Álvarez-Camacho M, Gonella S, Campbell S, Scrimger RA, Wismer WV. A systematic review of smell alterations after radiotherapy for head and neck cancer. Cancer Treat Rev. 2017 Mar;54:110–21.
7. Valentini MC, Mellai M, Annovazzi L, Melcarne A, Denysenko T, Cassoni P, et al. Comparison among conventional and advanced MRI, 18F-FDG PET/CT, phenotype and genotype in glioblastoma. :18.
8. Stockham AL, Tievsky AL, Koyfman SA, Reddy CA, Suh JH, Vogelbaum MA, et al. Conventional MRI does not reliably distinguish radiation necrosis from tumor recurrence after stereotactic radiosurgery. J Neurooncol. 2012 Aug;109(1):149–158.
9. Soffietti R, Rudā R, Mutani R. Management of brain metastases. J Neurol. 2002 Oct;249(10):1357–1369.
10. Hassanzadeh C, Rao YJ, Chundury A, Rowe J, Ponisio MR, Sharma A, et al. Multiparametric MRI and [18F]Fluorodeoxyglucose Positron Emission Tomography Imaging Is a Potential Prognostic Imaging Biomarker in Recurrent Glioblastoma. Front Oncol. 2017;7:178.
11. Houshmand S, Salavati A, Segtnan EA, Grupe P, Høilund-Carlsen PF, Alavi A. Dual-time-point Imaging and Delayed-time-point Fluorodeoxyglucose-PET/Computed Tomography Imaging in Various Clinical Settings. PET Clin. 2016 Jan;11(1):65–84.
12. Prieto E, Marti-Climent JM, Dominguez-Prado I, Garrastachu P, Diez-Valle R, Tejada S, et al. Voxel-Based Analysis of Dual-Time-Point 18F-FDG PET Images for Brain Tumor Identification and Delineation. J Nucl Med. 2011 Jun;52(6):865–872.
13. Roppongi M, Izumisawa M, Terasaki K, Muraki Y, Shozushima M. 18F-FDG and 11C-choline uptake in proliferating tumor cells is dependent on the cell cycle in vitro. Ann Nucl Med. 2019;33(4):237–43.
14. Cho E, Rubinstein L, Stevenson P, Gooley T, Philips M, Halasz LM, et al. The use of stereotactic radiosurgery for brain metastases from breast cancer: Who benefits most? Breast Cancer Res Treat. 2015 Feb;149(3):743–749.
15. Larroza A, Moratal D, Paredes-Sánchez A, Soria-Olivas E, Chust ML, Arribas LA, et al. Comment on “Computer-Extracted Texture Features to Distinguish Cerebral Radionecrosis from Recurrent Brain Tumors on Multiparametric MRI: A Feasibility Study.” Am J Neuroradiol. 2017;38(3):E21–E21.
16. Chukwueke UN, Wen PY. Use of the Response Assessment in Neuro-Oncology (RANO)

criteria in clinical trials and clinical practice. CNS Oncol [Internet]. 2019 Feb 26 [cited 2020 Sep 28];8(1). Available from: https://www.ncbi.nlm.nih.gov/pmc/articles/PMC6499019/
17. SPM - Statistical Parametric Mapping [Internet]. [cited 2020 Sep 28]. Available from: https://www.fil.ion.ucl.ac.uk/spm/
18. Chris Rorden's Neuropsychology Lab | CRNL [Internet]. [cited 2020 Sep 28]. Available from: https://www.mccauslandcenter.sc.edu/crnl/chris-rordens-neuropsychology-lab
19. Horky LL, Hsiao EM, Weiss SE, Drappatz J, Gerbaudo VH. Dual phase FDG-PET imaging of brain metastases provides superior assessment of recurrence versus post-treatment necrosis. J Neurooncol. 2011;103(1):137–146.
20. Delishaj D, Ursino S, Pasqualetti F, Pesaresi I, Desideri I, Cosottini M, et al. The Effectiveness of Bevacizumab in Radionecrosis After Radiosurgery of a Single Brain Metastasis. Rare Tumors [Internet]. 2015 Dec 29 [cited 2020 Sep 28];7(4). Available from: https://www.ncbi.nlm.nih.gov/pmc/articles/PMC4703924/
21. Delishaj D, Ursino S, Pasqualetti F, Cristaudo A, Cosottini M, Fabrini MG, et al. Bevacizumab for the Treatment of Radiation-Induced Cerebral Necrosis: A Systematic Review of the Literature. J Clin Med Res. 2017 Apr;9(4):273–80.
22. Narloch JL, Farber SH, Sammons S, McSherry F, Herndon JE, Hoang JK, et al. Biopsy of enlarging lesions after stereotactic radiosurgery for brain metastases frequently reveals radiation necrosis. Neuro-Oncol. 2017 Oct;19(10):1391–1397.
23. Kim Y-I, Cho KG, Jang SJ. Comparison of dual-time point 18F-FDG PET/CT tumor-to-background ratio, intraoperative 5-aminolevulinic acid fluorescence scale, and Ki-67 index in high-grade glioma. Medicine (Baltimore). 2019 Feb;98(8):e14397.
24. Leiva-Salinas C, Muttikkal TJE, Flors L, Puig J, Wintermark M, Patrie JT, et al. FDG PET/MRI Coregistration Helps Predict Response to Gamma Knife Radiosurgery in Patients With Brain Metastases. AJR Am J Roentgenol. 2019;212(2):425–30.
25. Dunet V, Rossier C, Buck A, Stupp R, Prior JO. Performance of 18F-fluoro-ethyl-tyrosine (18F-FET) PET for the differential diagnosis of primary brain tumor: a systematic review and Metaanalysis. J Nucl Med Off Publ Soc Nucl Med. 2012 Feb;53(2):207–14.
26. Humbert O, Bourg V, Mondot L, Gal J, Bondiau P-Y, Fontaine D, et al. 18F-DOPA PET/CT in brain tumors: impact on multidisciplinary brain tumor board decisions. Eur J Nucl Med Mol Imaging. 2019;46(3):558–68.
27. Yu J, Zheng J, Xu W, Weng J, Gao L, Tao L, et al. Accuracy of 18F-FDOPA Positron Emission Tomography and 18F-FET Positron Emission Tomography for Differentiating Radiation Necrosis from Brain Tumor Recurrence. World Neurosurg. 2018 Jun;114:e1211–24.
28. Huhdanpaa H, Hwang DH, Gasparian GG, Booker MT, Cen Y, Lerner A, et al. Image Coregistration: Quantitative Processing Framework for the Assessment of Brain Lesions. J Digit Imaging. 2014 Jun;27(3):369–79.

Annexes

Annexe 1

Annexe 1 : MRI reconstruction protocols and parameters										
Sequence	Acquisition time	voxel size (mm3)	PAT factor	TR (ms)	TE (ms)	Interslice gap (yes/non)	BW (Hz/pixel)	Inversion time (ms)	slices	slice thickness (mm)
3D-T1 MPRAGE	4 min 40 s	0.9×0.9×0.9	2	2000	2,19	no	220	900	192	0,9
3D-FLAIR	5 min 02 s	0.5×0.5×1.1	2	5000	400	no	781	1800	144	1,1
ASL	4 min 55 s	3.4×3.4×4.0	2	4350	20,86	no	2442		24	4
ENC Perfusion	2 min 21 s	1.7×1.7×3.5	2	1800	30	no	2056		30	3,5
Permeability	1 min 13 s	1.2×1.2×3.0	2	4,02	1,42	no	390		48	3

Annexe 2

Coregistration quantitative analysis

No	Variable	Progression group	Radionecrosis group	Estimation*	95% CI	p	Adjusted p-value	Test*
1	ROI MRI PerfusionWeighted	209.54	262.58	4.95	(-353.28 -- 338.93)	.99	.99	WMW
2	ROI MRI relCBF	86.35	70.60	15.74	(-15.05 -- 46.54)	.275	.754	Welch
3	ROI MRI TTP	28.89	28.52	-0.37	(-3265.2 -- 10.06)	.833	.932	WMW
4	ROI MRI MTT	7.27	8.05	-0.95	(-1342.76 -- 1.86)	.524	.754	WMW
5	ROI MRI rBF	24.13	26.37	-2.98	(-80.62 -- 10.81)	.622	.802	WMW
6	ROI MRI rBV	2.78	4.83	-2.08	(-188.4 -- 1.11)	.181	.754	WMW
7	ROI MRI TMAX	3.43	4.99	-1.17	(-7.2 -- 10.04)	.648	.802	WMW
8	ROI MRI K2	231.77	157.98	73.79	(-102.92 -- 250.51)	.354	.754	Welch
9	ROI MRI tMIP	358.71	356.86	1.84	(-109.33 -- 113.02)	.97	.99	Welch
10	ROI MRI rBVcorrected	1.78	2.17	-0.39	(-1.34 -- 0.58)	.377	.754	Welch

11	ROI MRI VE	56.06	188.34	-21.56	(-195.84 -- 88.62)	.527	.754	WMW
12	ROI MRI VP	40.75	60.84	-20.09	(-64.71 -- 24.53)	.282	.754	Welch
13	ROI MRI KTRANS	124.13	138.55	-14.42	(-106.44 -- 77.61)	.721	.848	Welch
14	ROI MRI KEP	724.31	889.77	-89.94	(-1520.76 -- 6875.92)	.412	.754	WMW
15	ROI MRI AUC	4919.55	9898.42	-3796.70	(-19511.55 -- 9673.48)	.648	.802	WMW
16	ROI MRI Washin	0.82	0.99	-0.17	(-0.92 -- 0.59)	.556	.769	Welch
17	ROI MRI PEAK	21.32	50.40	-16.42	(-80.08 -- 44.54)	.412	.754	WMW
18	ROI MRI Washout	1589.29	560.87	1028.42	(-536.38 -- 2593.23)	.167	.754	Welch
19	ROI MRI TME	118.74	131.34	-12.60	(-47.73 -- 22.54)	.437	.754	Welch
20	ROI MRI SER	223.76	201.84	21.92	(-45.39 -- 89.23)	.473	.754	Welch
21	ROI MRI PeakEnhancement	21.76	34.50	-12.74	(-38.83 -- 13.36)	.259	.754	Welch
22	ROI MRI CurveWashout	12.49	15.48	-2.99	(-13.52 -- 7.54)	.53	.754	Welch
23	ROI MRI / WM PerfusionWeighted	0.85	1.05	-0.19	(-1.16 -- 0.78)	.628	.802	Welch

24	ROI MRI / WM relCBF	0.84	0.66	0.18	(-0.36 -- 0.73)	.424	.754	Welch
25	ROI MRI / WM TTP	1.06	0.98	0.08	(-0.11 -- 0.28)	.35	.754	Welch
26	ROI MRI / WM MTT	1.05	1.05	-0.00	(-0.49 -- 0.49)	.989	.99	Welch
27	ROI MRI / WM rBF	1.56	1.39	0.16	(-0.35 -- 0.68)	.472	.754	Welch
28	ROI MRI / WM rBV	1.91	1.97	-0.05	(-1.03 -- 0.93)	.904	.989	Welch
29	ROI MRI / WM TMAX	3.21	2.38	0.83	(-1.95 -- 3.63)	.513	.754	Welch
30	ROI MRI / WM K2	5.62	14.64	-5.50	(-29.64 -- 2428.76)	.413	.754	WMW
31	ROI MRI / WM tMIP	1.64	1.64	-0.01	(-0.54 -- 0.54)	.974	.99	Welch
32	ROI MRI / WM rBVcorrected	1.61	1.86	-0.26	(-0.59 -- 0.51)	.315	.754	WMW
33	ROI MRI / WM VE	9.61	14.10	-4.49	(-15.6 -- 6.63)	.372	.754	Welch
34	**ROI MRI / WM VP**	**2.10**	**3.48**	**-1.38**	**(-2.68 -- -0.07)**	**.042**	**.391**	**Welch**
35	ROI MRI / WM KTRANS	2.52	4.92	-2.39	(-5.08 -- 0.3)	.073	.569	Welch

36	ROI MRI / WM KEP	0.98	0.88	0.10	(-0.5 -- 0.71)	.704	.848	Welch
37	ROI MRI / WM AUC	3.16	7.41	-4.17	(-8.63 -- 2.27)	.23	.754	WMW
38	**ROI MRI / WM Washin**	**1.45**	**2.30**	**-0.85**	**(-1.61 -- -0.09)**	**.035**	**.391**	**Welch**
39	ROI MRI / WM PEAK	2.28	5.85	-2.98	(-4.41 -- 1.96)	.109	.732	WMW
40	ROI MRI / WM Washout	1.80	10.08	-3.28	(-29.04 -- 13.21)	.412	.754	WMW
41	ROI MRI / WM TME	1.61	1.70	-0.09	(-0.92 -- 0.75)	.814	.932	Welch
42	ROI MRI / WM SER	0.68	0.76	-0.08	(-0.33 -- 0.19)	.525	.754	Welch
43	**ROI MRI / WM PeakEnhancement**	**2.66**	**4.60**	**-1.94**	**(-3.71 -- -0.16)**	**.037**	**.391**	**Welch**
44	ROI MRI / WM CurveWashout	8.27	13.61	-5.34	(-16.97 -- 6.29)	.307	.754	Welch
45	ROI Early / WM	1.25	1.01	0.24	(-0.11 -- 0.59)	.166	.754	Welch
46	**ROI Delayed / WM**	**2.10**	**1.10**	**1.00**	**(0.33 -- 1.67)**	**.008**	**.361**	**Welch**
47	**Retention Index**	**0.72**	**0.10**	**0.62**	**(0.14 -- 1.1)**	**.016**	**.374**	**Welch**

*The colon Est is an estimation of the median of the differences (in case of a Wilcoxon-Mann-Whitney test) or the differences of the means (in case of a Welsh test) between the two groups tumor progression and radionecrosis.
Differences with statistical significance (α = .05) are in bold.
ROIs : **MRI** (ROI drawn on the T1 MPRAGE images), **Early** (ROI drawn on the early one hour PET), **Delayed** (ROI drawn on the delayed four hour PET) and **WM** (ROI drawn on contralateral white matter)
No : Number of metric
No 1 to 22 : metric recorded inside the **MRI** ROI, drawn on the T1 MPRAGE images
No 23 to 44 : standardized metrics **MRI** / **ROI**
Retention Index = [(**Delayed**/**WM** - **Early**/**WM**)/(**Early**/**WM**)]

SERMENT D'HIPPOCRATE

Au moment d'être admis(e) à exercer la médecine, je promets et je jure d'être fidèle aux lois de l'honneur et de la probité.
Mon premier souci sera de rétablir, de préserver ou de promouvoir la santé dans tous ses éléments, physiques et mentaux, individuels et sociaux.
Je respecterai toutes les personnes, leur autonomie et leur volonté, sans aucune discrimination selon leur état ou leurs convictions. J'interviendrai pour les protéger si elles sont affaiblies, vulnérables ou menacées dans leur intégrité ou leur dignité. Même sous la contrainte, je ne ferai pas usage de mes connaissances contre les lois de l'humanité.

J'informerai les patients des décisions envisagées, de leurs raisons et de leurs conséquences.
Je ne tromperai jamais leur confiance et n'exploiterai pas le pouvoir hérité des circonstances pour forcer les consciences.

Je donnerai mes soins à l'indigent et à quiconque me les demandera. Je ne me laisserai pas influencer par la soif du gain ou la recherche de la gloire.

Admis(e) dans l'intimité des personnes, je tairai les secrets qui me seront confiés. Reçu(e) à l'intérieur des maisons, je respecterai les secrets des foyers et ma conduite ne servira pas à corrompre les moeurs.
Je ferai tout pour soulager les souffrances. Je ne prolongerai pas abusivement les agonies. Je ne provoquerai jamais la mort délibérément.

Je préserverai l'indépendance nécessaire à l'accomplissement de ma mission. Je n'entreprendrai rien qui dépasse mes compétences. Je les entretiendrai et les perfectionnerai pour assurer au mieux les services qui me seront demandés.

J'apporterai mon aide à mes confrères ainsi qu'à leurs familles dans l'adversité.

Que les hommes et mes confrères m'accordent leur estime si je suis fidèle à mes promesses ; que je sois déshonoré(e) et méprisé(e) si j'y manque.

SERMENT D'HIPPOCRATE

En présence des Maîtres de cette FACULTE et de mes chers CONDISCIPLES, je promets et je jure d'être fidèle aux lois de l'Honneur et de la Probité dans l'exercice de la Médecine.

Je donnerai mes soins gratuits à l'indigent et je n'exigerai jamais un salaire au-dessus de mon travail. Admis dans l'intérieur des maisons, mes yeux ne verront pas ce qui s'y passe, ma langue taira les secrets qui me seront confiés et mon état ne servira pas à corrompre les moeurs ni à favoriser le crime.

Respectueux et reconnaissant envers mes MAÎTRES, je rendrai à leurs enfants l'instruction que j'ai reçue de leurs pères.

Que les HOMMES m'accordent leur estime si je suis fidèle à mes promesses. Que je sois couvert d'OPPROBRE et méprisé de mes confrères si j'y manque.

Intérêt d'une évaluation hybride en TEP FDG dynamique et IRM de perfusion pour le diagnostic différentiel entre progression et radionécrose dans les lésions cérébrales traitées par radiothérapie stéréotaxique.

RÉSUMÉ :

INTRODUCTION : La TEP 18FDG cérébrale biphasique (TEP) est une technique robuste pour évaluer les lésions cérébrales, le traceur s'accumulant dans les métastases ou récidives locales et restant stable dans le cortex ou les processus inflammatoires, permettant ainsi de différencier les récidives tumorales (TR) des radionécroses (RN) sur les métastases cérébrales (MC) traitées par radiothérapie stéréotaxique (SRS). La corégistration des données d'IRM et TEP permettrait alors d'extraire des biomarqueurs diagnostiques pertinents.

OBJECTIF : Déterminer des biomarqueurs IRM et TEP associés au diagnostic de TR ou RN chez des patients traités par SRS sur MC.

METHODE : 15 patients traités par SRS pour MC ont été rétrospectivement inclus sur 2 hôpitaux français. Leur IRM de fin de traitement n'a pas pu distinguer RN et TR. Chaque patient a bénéficié d'une IRM et d'une TEP 3 mois après leur traitement. Ces examens ont été analysés quantitativement et visuellement en aveugle des interprétations initiales. La TEP biphasique consistait en une acquisition «précoce» et «tardive» respectivement 1 et 4 heures après injection. Des régions d'intérêt tumorales (ROI) ont été tracées sur les différentes séquences TEP et IRM ainsi qu'une ROI miroir de référence controlatérale pour standardisation. Chaque métrique calculée à l'intérieur de ces ROIs a été analysée quantitativement, notamment le SUVmax ainsi que sa variation dans le temps. Une augmentation de 20% du SUVmax était retenue comme évocatrice de TR. Le diagnostic final était basé sur la décision de la réunion de concertation pluridisciplinaire à 6 mois de la TEP.

RESULTATS : 9 patients étaient en récidive locale et 6 en radionécrose. L'analyse semi-quantitative TEP et IRM retrouvait respectivement 100% et 77,8% de Sensibilité et 100% et 83,3% de Spécificité. Une augmentation de 20% du SUVmax traduisait une TR. Après standardisation, il y avait une différence significative entre les deux groupes pour les métriques VP, Washin, Peak Enhancement ainsi que l'évolution du SUVmax tumoral standardisé.

CONCLUSION : La TEP biphasique discrimine efficacement entre TR et RN. L'analyse conjointe des données TEP et IRM améliore la précision diagnostique.

Mots- clés :

- TEP FDG double phase
- radiothérapie stéréotaxique
- métastase cérébrale
- IRM
- corégistration
- radionécrose